



Published in final edited form as:

Curr Biol. 2008 November 25; 18(22): 1785–1791. doi:10.1016/j.cub.2008.11.007.

Kinetochore attachments require an interaction between unstructured tails on microtubules and Ndc80^{Hec1}

Stephanie A. Miller¹, Michael L. Johnson², and P. Todd Stukenberg^{1,*}

¹Department Biochemistry and Molecular Genetics, University of Virginia School of Medicine, Charlottesville, Virginia 22908

²Departments of Pharmacology and Medicine, University of Virginia School of Medicine, Charlottesville, Virginia 22908

Summary

Kinetochores bind and regulate the plus-ends of microtubules during mitosis. These attachments must be tight enough to move chromosomes, while the microtubule end both remains dynamic and repositions within the attachment pocket so that connections are maintained during depolymerization. Hec1/Ndc80 (Hec1) is a subunit of the four-protein Ndc80 complex, which is an important structural component of the kinetochore [1-3]. Kinetochores are unable to bind microtubules after Hec1 knockdown [2,4]; however, because the Ndc80 complex has structural roles, it is unclear if Hec1 directly mediates kinetochore microtubule attachments. Hec1 has a microtubule-binding site composed of both an unstructured N-terminal tail and a calponin homology domain [5-7]. Here we show that, surprisingly, the N-terminal tail is sufficient for microtubule binding affinity in vitro. The interaction is salt sensitive and the positively charged Hec1 tail is unable to bind microtubules lacking negatively charged tails. We have replaced the endogenous Hec1 subunit with a mutant lacking the N-terminal tail. These cells assemble kinetochores properly but are unable to congress chromosomes, generate tension across sister kinetochores, or establish cold-stable kinetochore-microtubule attachments. Our data argue that the highest affinity interactions between kinetochores and microtubules are ionic attractions between two unstructured domains. We discuss the importance of this finding for models of repositioning of microtubules in the kinetochore during depolymerization.

Keywords

mitotic spindle; Hill sleeve; chromosome; congression; mitosis

Results

How a kinetochore can generate microtubule attachments strong enough to move chromosomes but also control microtubule dynamics is an important question. Kinetochores contain greater than 60 proteins including over 10 that can directly interact with microtubules in vitro [8]. The Ndc80 complex is localized to kinetochores and is important for most kinetochore functions. It contains four subunits Hec1/Ndc80 (Hec1), Nuf2, Spc24 and Spc25 [3,9]. The N-terminus of Hec1 can directly bind microtubules and the complex is required to generate stable microtubule attachments and congress chromosomes in all tested model systems [8]. However, the direct contribution of the Ndc80 complex to these functions is confounded by its structural role at kinetochores. Vertebrate kinetochores

*Corresponding author: Tel: (434) 924-5253, Fax: (434) 924-5069, pts7h@virginia.edu.

cannot assemble most outer kinetochore and fibrous corona proteins after depletion of the Ndc80 complex including Zwint1, Rod, ZW10, Dynein, Dynactin, Mad1, and Mad2 [2,3,10]. Moreover, the outer plate kinetochore structure that is seen by conventional electron microscopy is highly disorganized after siRNA knockdown of the Nuf2 subunit [1].

The crystal structure of an engineered Ndc80 complex has recently been solved [6]. Hec1 has an 80 amino acid unstructured tail, followed by a calponin homology domain (CHD). Hec1 then interacts with Nuf2 through a long coiled-coil. The C-termini of this dimer forms a tetramerization domain with the N-terminal coils of Spc24 and Spc25 [11]. Interestingly, the N-terminus of Nuf2 also contains a CHD [6]. Within the kinetochore, the Ndc80 complex is oriented with the Spc24/Spc25 globular heads toward the inner kinetochore and the double CHD formed by Ndc80/Nuf2 extending outward [12]. Because the calponin homology domain is also found in a classic plus end tip tracking protein, EB1 [13], most models suggest that this is the critical domain for microtubule attachment. Formal proof of this model requires identifying mutants of the Ndc80 complex that assemble kinetochores but do not bind microtubules.

The Ndc80 complex directly binds microtubules in vitro. The affinity of *S.cerevisiae* Ndc80/Nuf2 dimer is reduced 10-fold when the Ndc80 N-terminal tail is removed [7] and similarly in an engineered human Ndc80 complex the deletion of the Hec1 tail reduces microtubule binding 100-fold [6]. Point mutations of the Hec1 CHD also reduce microtubule binding, albeit to a lesser extent than the tail deletion. We were interested in whether the N-terminal tail participates with the CHD to generate a binding site or if the tail binds microtubules on its own. To distinguish between these models we used the following recombinant proteins: the N-terminus of Hec1 containing both the tail and CHD (Hec1 1-230), the CHD only (Hec1 81-230), and the tail only (Hec1 1-80) (Supplemental Figure 1). 100nM of each recombinant Hec1 protein was incubated with increasing concentrations of taxol-stabilized microtubules (100nM to 6 μ M) in a buffer containing physiological salt concentrations and sedimented through a glycerol cushion to separate microtubule bound from unbound Hec1. Supernatant and pellet samples were collected and analyzed by Western blotting (Figure 1A). We generated a peptide antibody against amino acids 48-71 of Hec1 to detect Hec1(1-80) (Supplemental Figure 4). The amount of Hec1 bound to microtubules was expressed as the percentage of Hec1 signal in the pellet compared to the total amount of Hec1 (Figure 1B). The Ndc80 complex displays cooperativity in binding to microtubules [5,6] and therefore to analyze the binding data and accurately calculate apparent K_d values for Hec1, we used a modified Hill equation. Hec1(1-230) bound to microtubules with an apparent K_d of 1.02 μ M \pm 0.18 (95% confidence). The N-terminal tail, Hec1(1-80), was able to bind tubes with an apparent K_d of 0.64 μ M \pm 0.08. Although there was a slight statistical difference in the apparent K_d of Hec1(1-230) and Hec1(1-80), both proteins bound microtubules with similar kinetics and cooperativity. The CHD alone poorly bound microtubules even at high microtubule concentrations. Our data indicates that the N-terminal tail is the predominant in vitro microtubule-binding motif on Hec1.

The N-terminal tail of Hec1 contains 15 positively charged amino acids (net 10 positive charges at neutral pH). In contrast both α and β tubulin subunits have negatively charged unstructured C-terminal tails (β 1 subunit has 10 negative charges). We tested whether Hec1 requires the tubulin tails to bind microtubules. We digested taxol-stabilized microtubules with subtilisin to produce microtubules lacking the β -tubulin tail (Supplemental Figure 2A) [14]. In co-sedimentation assays, none of the Hec1 proteins were able to bind to tail-less microtubules (Supplemental Figure 2B) as seen previously[6]. The subtilisin-digested microtubules were able to sediment as well as those formed with undigested tubulin (Supplemental Figure 2C). We conclude that Hec1 interacts with the C-terminal tail of tubulin. Increasing the salt concentration from 100mM to 200mM KCl abolished almost all

microtubule binding of Hec1(1-230) and Hec1(1-80) (Figure 1C) demonstrating that the interaction between the Hec1 tail and the tails of microtubules is based on ionic attraction.

It is possible that the tail interacts with both the microtubule and the CHD. To test this we titrated Hec1(1-80) into a microtubule binding assay with 100nM Hec1(81-230) and 6 μ M tubulin. We could not identify a concentration of Hec1(1-80) that was able to increase the binding of the CHD to microtubules arguing for independent binding affinities for the two domains (Supplemental Figure 3).

To determine the significance of the microtubule binding by the N-terminal tail, we developed a protocol to deplete endogenous Hec1 by siRNA and express siRNA-insensitive Hec1 (WT rescue) or Hec1 lacking the N-terminal tail (Δ N rescue). HeLa cells were synchronized by double thymidine block and transfected with siRNA and rescue plasmid as outlined in Figure 2A. This ensured that we observed the first mitosis after Hec1 replacement and generated a large population of cells traversing mitosis. Hec1 protein levels were reduced >95% as detected by Western blot. Nuf2 was also reduced to about 95% while Spc24 and Spc25 levels did not change after Hec1 siRNA (Supplemental Figure 5B).

Because Hec1 plays a structural role in the kinetochore, we first determined if proteins mislocalized after Hec1 siRNA, were assembled onto kinetochores after expression of WT Hec1 or the Δ N mutant. Kinetochore assembly was measured by immunofluorescence and expressed as the ratio between the kinetochore protein staining and ACA staining. Only cells that regained endogenous Hec1 staining levels were analyzed (Figure 2C). Nuf2 protein levels are reduced after Hec1 siRNA by Western blotting and, as expected, Nuf2 signal is not seen at kinetochores in cells depleted of Hec1 (Supplemental Figure 6). Nuf2 signal was restored in WT and Δ N transfected cells but due to the background signal the extent of localization rescue could not be quantified. Interestingly, Spc24 and Spc25, thought to be the kinetochore-targeting subunits of the Ndc80 complex, do not localize to kinetochores after Hec1 siRNA (Figure 2B) even though the protein levels are unchanged (Supplemental Figure 5B). Spc24 and Spc25 kinetochore staining is restored to control levels when either Hec1 WT or the Δ N mutant are expressed (Figure 2C). These cells were also immunostained for anti-centromere antigen (ACA), a marker of inner kinetochores, Mad2, a spindle checkpoint protein, Knl1, a microtubule binding protein, Nnf1, a member of the Mis 12 complex, CENP-F, a fibrous corona protein, and Rod, a member of the RZZ complex (Figure 2B). Both WT and Δ N rescue restored the localization of Mad2, CENP-F and Rod to control levels (Figure 2C). Knl-1 and Nnf1 were present when Hec1 was depleted and were not displaced after either the WT or Δ N rescue (Figure 2B). We conclude that the kinetochore is intact when Hec1 depleted cells are rescued by either WT or Δ N Hec1.

To determine if the N-terminal tail is required for kinetochore-microtubule attachments in vivo, we analyzed cells rescued for Hec1 expression for spindle morphology and chromosome alignment by immunofluorescent staining of cells for tubulin, Hec1, and ACA. Cells depleted of Hec1 and rescued with EGFP as a control (siHec1) showed characteristic phenotypes of Hec1 knock-down including increased spindle length, and poor chromosome congression (Figure 3A). Chromosome congression was quantified as the percentage of mitotic cells that were able to align chromosomes to produce a metaphase plate in three independent experiments (Figure 3B). $38.3 \pm 0.04\%$ of control cells were in metaphase which was reduced to $1.9 \pm 0.02\%$ in siHec1 cells. This phenotype is rescued in cells expressing WT Hec1 but not the Δ N mutant. $38.3 \pm 0.06\%$ of WT rescue cells were in metaphase, while only $1.3 \pm 0.02\%$ of Δ N rescue cells were in metaphase. The kinetochore is not able to align chromosomes without the N-terminal tail of Hec1.

Kinetochores microtubule attachments generate tension and separate sister kinetochores. As a readout for stable attachment, we measured the interkinetochore distance between sister chromatids in cells expressing different Hec1 proteins. For each rescue condition, 10 kinetochores were measured in 10 cells for both early prometaphase and metaphase from three independent experiments. Late prometaphase cells often had tilted spindles such that sister kinetochores were rarely in the same focal plane making distance measurements difficult. Control cells had an average interkinetochore distance of $0.7 \pm 0.10 \mu\text{m}$ in prometaphase and $1.6 \pm 0.21 \mu\text{m}$ in metaphase (Figure 3C). Cells rescued with WT Hec1 had similar interkinetochore distances in both prometaphase and metaphase, $0.8 \pm 0.12 \mu\text{m}$ and $1.4 \pm 0.09 \mu\text{m}$, respectively. Hec1 depleted cells were all in prometaphase and had an average interkinetochore distance of $1.0 \pm 0.05 \mu\text{m}$, similar to that of control cells in nocodazole ($0.9 \pm 0.10 \mu\text{m}$). Since the ΔN rescue cells were unable to align chromosomes and had Mad2 staining on the majority of kinetochores (not shown) they were scored as prometaphase and had an average interkinetochore distance of $1.0 \pm 0.06 \mu\text{m}$. Interkinetochore distances in siHec1 and ΔN rescue cells are slightly higher than that of control and WT rescue cells in early prometaphase. This is most likely due to dynein which is active at kinetochores even when the binding activity of Hec1 is blocked [15]. The kinetochore is not able to generate interkinetochore tension without the N-terminal tail of Hec1.

Most microtubules depolymerize when cells are lysed in ice-cold buffer; however, microtubules embedded in the outer kinetochore plate or pole to pole microtubules are resistant to this treatment. Cells were incubated in ice-cold media for 10 minutes prior to fixation and then processed for immunofluorescence for Hec1, tubulin, and ACA. Stable attachments were scored by quantifying the number of kinetochores that had bundles of associated tubulin in early prometaphase, late prometaphase, and metaphase (Figure 4A). 10 kinetochores were scored from 5 or more cells for each condition in two independent experiments. In control HeLa cells the percent of kinetochores that had associated tubulin bundles increased as they traversed mitosis; $26 \pm 18\%$ in early prometaphase, $98.4 \pm 3.9\%$ in late prometaphase, and $100 \pm 0.0\%$ in metaphase (Figure 4B). Similarly, WT rescue kinetochores were found to have cold stable microtubules that end at kinetochores in $23.2 \pm 13.1\%$ in early prometaphase, $97.2 \pm 4.2\%$ in late prometaphase, and $98.8 \pm 1.9\%$ in metaphase. In contrast, only $3.1 \pm 3.3\%$ of kinetochores in Hec1 depleted cells had associated microtubules, and this was only slightly increased in ΔN rescue cells at $10.5 \pm 6.5\%$. The N-terminus of Hec1 is required to form stable kinetochore-microtubule attachments.

Discussion

After loss of Ndc80 complex function, cells from all tested species lose end-on attachments and the chromosome movements powered by the depolymerization of microtubules [16]. It was unclear in all of these studies if these phenotypes were caused by structural or direct roles of the complex. Our data argue that the unstructured N-terminal tail of Hec1 directly binds the unstructured C-terminal tails of tubulin. Cells knocked down of the endogenous Hec1 and expressing a mutant lacking this microtubule binding motif were unable to productively bind microtubules, generate interkinetochore tension or congress chromosomes. The lack of microtubule attachments was not caused by improper kinetochore assembly. Ten different proteins, representing different areas of the kinetochore all localize to endogenous levels in cells expressing this Hec1 ΔN mutant. We conclude that the Hec1 ΔN mutant separates the structural and microtubule binding roles of the protein and our data argue strongly that the Hec1 tail is the critical attachment point for depolymerization-coupled movements of chromosomes.

How can the interactions between an unstructured tail on microtubules and a second one on Hec1 generate a tight enough interface to move a chromosome? The microtubule tails are highly negatively charged (i.e. 10 acidic amino acids in β 1) and the Hec1 tail contains 15 basic amino acids and a net charge of +10. The interaction is ionic since it is salt sensitive. Although the two tails can tightly interact at physiological salt (100mM KCl), the interaction was lost when the binding assays were performed in 200 mM KCl. Kinetochores are thought to contain at least 8 Hec1 proteins per microtubule [17] generating the potential for 80 ionic interactions on a single microtubule or approximately 1600 per human kinetochore. Further experimentation is required to clarify whether these tails remain unstructured after binding or if they form a structured binding interface.

In 1985, Hill proposed that kinetochores could bind microtubules through a large number of weak interactions between the kinetochore and the lateral sides of the microtubule plus end [18]. He demonstrated mathematically that such a sleeve could allow repositioning of the microtubule during depolymerization, while simultaneously generating the force needed for chromosome movement. Our data provide the first working model for a “Hill-sleeve”. We propose that the unstructured tails of Hec1 and microtubules bind through numerous charge based interactions. Moreover chromosome repositioning would be powered by burying the positive charge of Hec1 tails that would become exposed as microtubules depolymerize. The flexibility of unstructured tails could facilitate the repositioning of microtubules, by allowing movement while maintaining attachment.

The calponin homology domains are still present in our Δ N mutant and thus are not sufficient for stable microtubule binding *in vivo*. However, our experiments do not suggest that the CHD of Hec1 is unimportant. Although under our conditions the CHD cannot bind microtubules, a recent study argues that the CHD can contribute to *in vitro* binding when the tail is present [6]. These studies contained Nuf2 and Hec1 CHDs, lower salt and 10-fold higher concentrations of proteins all of which may drive protein interactions. At kinetochores the local concentration of the Ndc80 complex and microtubules may be high enough for the CHD to productively bind on its own. Future studies must be directed towards understanding if the unstructured tail of Hec1 and the CHD work together to generate a mature attachment site and mediate depolymerization-coupled movements.

Experimental Procedures

Recombinant Protein Expression and Purification

Hec1 WT (aa1-230), Hec1 Δ N (aa81-230), and Hec1 N-term (aa1-80) were cloned into pET28a and purified on Ni-NTA agarose (Qiagen). All recombinant proteins were exchanged into dilution buffer (100mM KCl, 10mM Na-HEPES, 1mM EDTA, 1mM DTT, 1mM MgCl₂, 0.1 M CaCl₂, 10% glycerol).

Microtubule Polymerization and Subtilisin Digestion

PC-tubulin was polymerized to microtubules as previously described [19]. To cleave primarily β -tubulin tails, microtubules were digested with subtilisin A (Sigma) at 1:100 (w/w) for 30 min at 37°C and quenched with 1mM PMSF for 30 min at 30°C. Microtubules were resuspended in dilution buffer supplemented with 40uM taxol.

Microtubule Cosedimentation Assays

Cosedimentation assays were performed in dilution buffer with 10 μ M taxol as previously described [5].

Western Blotting, Slot Blotting and Quantification

For determining Hec1 knockdown levels and microtubule binding, Western blotting was performed as previously described [3]. For slot blotting, supernatant and pellet samples in SDS sample buffer were diluted to 500 μ l in PBS and transferred to immobilon membrane (Millipore) using a Minifold I Microsample Filtration Manifold (Schleicher and Schuell). WT and Δ N proteins were immunodetected by anti-Hec1 (GTX70268, GeneTex) and the Hec1 N-term (aa1-80) was detected by anti-Hec1(48-71). The Hec1 peptide antibody was produced as previously described [20]. Densitometry was carried out with ImageQuant TL (Amersham Biosciences). Percent Hec1 bound to microtubules was expressed as pellet signal divided by total supernatant and pellet signal. Mean binding values from three independent experiments were used to determine apparent K_d by nonlinear least-squares fitting of a modified Hill equation:

$$Y = \frac{B_{\max}(X - Y)^h}{(K_d + (X - Y)^h)}$$

where B_{\max} = the maximum specific binding, Y = the bound concentration, X = total concentration, h = the hill slope, and K_d = the concentration for half maximum binding. The substitution of the total minus the bound concentration (X-Y) to represent the unbound concentration allows the Hec1 and tubulin to be of comparable magnitude. The amount bound was then calculated with a numerical root finder. The 95% confidence intervals of the resulting parameter values were determined by a bootstrap method.

Cell Culture

HeLa cells (ATCC) were maintained in Dulbecco's Modified Eagle's Medium (Invitrogen) supplemented with 10% fetal bovine serum in a humidified incubator at 37°C with 5% CO₂. For synchronization, cells were seeded in media containing 2mM thymidine for 24-36 hours, released into fresh media for 12 hours, arrested again in 2mM thymidine for 12 hours, released for 12 hours, and fixed for immunofluorescence. Hec1 siRNA sequence was used as previously described [21]. For rescue expression, all FLAG-Hec1 constructs were rendered insensitive to siRNA by changing four wobble bases in the siRNA targeted sequence (forward primer 5'GGAAATTGCTAGAGTGGAGCTTGAGTGTGAAACAATAAAA and reverse primer 5'TTTTATTGTTTCACACTCAAGCTCCACTCTAGCAATTTCC). For rescue experiments, cells were transfected with Lipofectamine 2000 (Invitrogen) at the first thymidine release with siRNA and rescue plasmid. Cells were transfected again at the second thymidine block with siRNA using RNAiMax (Invitrogen).

Immunofluorescence

Coverslips were co-fixed and extracted in PHEM buffer containing 2% paraformaldehyde and 0.5% Triton-X 100 for 20 min at room temperature or with ice cold 100% methanol for 10 min on ice. For cold lysis, cells were incubated on ice in cold media for 10 min before fixation with paraformaldehyde. Antibodies used were anti-Hec1, anti-Nuf2, anti-Spc24 and anti-Spc25[3], anti-ACA (Antibodies Incorporated), FITC conjugated anti-tubulin (DM1A, Sigma), anti-Nnf1 and anti-Knl1 (a gift from Arshad Desai), anti-CenpF and anti-Rod (a gift from Timothy Yen), and anti-Mad2 (a gift from Gary Gorbsky). The anti-Nuf2 polyclonal antibody was produced against the full length protein as previously described[22]. Immunostained cells were photographed with a spinning-disk confocal imaging system with a 63 \times 1.4NA Plan-Apochromatic Zeiss objective lens. The inverted microscope used was a Zeiss Axiovert 200 with a Perkin Elmer confocal attachment and a krypton/argon laser and

AOTF control to detect illumination at 488, 568, and 647nm. Digital images were obtained with a Hamamatsu digital CCD camera. Image acquisition, shutters, and z slices were all controlled using UltraView RS imaging software (Perkin Elmer).

Supplementary Material

Refer to Web version on PubMed Central for supplementary material.

Acknowledgments

We thank Dan Burke, Dan Foltz, and Gary Gorbsky for critical reading of the manuscript. SAM was trained under the Cell and Molecular Biology Training Grant from the University of Virginia. This work was funded by the America Cancer Society (RSG-04-021-01-CCG), the American Lung Foundation (P0759486), and the James and Rebecca Craig Foundation grant to the University of Virginia Cancer Center.

References

1. Deluca JG, Dong Y, Hergert P, Strauss J, Hickey JM, Salmon ED, McEwen BF. Hec1 and Nuf2 are Core Components of the Kinetochore Outer Plate Essential for Organizing Microtubule Attachment Sites. *Mol Biol Cell*. 2004
2. McClelland ML, Gardner RD, Kallio MJ, Daum JR, Gorbsky GJ, Burke DJ, Stukenberg PT. The highly conserved Ndc80 complex is required for kinetochore assembly, chromosome congression, and spindle checkpoint activity. *Genes Dev*. 2003; 17:101–114. [PubMed: 12514103]
3. McClelland ML, Kallio MJ, Barrett-Wilt GA, Kestner CA, Shabanowitz J, Hunt DF, Gorbsky GJ, Stukenberg PT. The vertebrate Ndc80 complex contains Spc24 and Spc25 homologs, which are required to establish and maintain kinetochore-microtubule attachment. *Curr Biol*. 2004; 14:131–137. [PubMed: 14738735]
4. Deluca JG, Moree B, Hickey JM, Kilmartin JV, Salmon ED. hNuf2 inhibition blocks stable kinetochore-microtubule attachment and induces mitotic cell death in HeLa cells. *J Cell Biol*. 2002; 159:549–555. [PubMed: 12438418]
5. Cheeseman IM, Chappie JS, Wilson-Kubalek EM, Desai A. The Conserved KMN Network Constitutes the Core Microtubule-Binding Site of the Kinetochore. *Cell*. 2006; 127:983–997. [PubMed: 17129783]
6. Ciferri C, Pasqualato S, Screpanti E, Varetto G, Santaguida S, Dos RG, Maiolica A, Polka J, De Luca JG, De WP, et al. Implications for kinetochore-microtubule attachment from the structure of an engineered Ndc80 complex. *Cell*. 2008; 133:427–439. [PubMed: 18455984]
7. Wei RR, Al Bassam J, Harrison SC. The Ndc80/HEC1 complex is a contact point for kinetochore-microtubule attachment. *Nat Struct Mol Biol*. 2007; 14:54–59. [PubMed: 17195848]
8. Cheeseman IM, Desai A. Molecular architecture of the kinetochore-microtubule interface. *Nat Rev Mol Cell Biol*. 2008; 9:33–46. [PubMed: 18097444]
9. Wigge PA, Kilmartin JV. The Ndc80p complex from *Saccharomyces cerevisiae* contains conserved centromere components and has a function in chromosome segregation. *J Cell Biol*. 2001; 152:349–360. [PubMed: 11266451]
10. Deluca JG, Howell BJ, Canman JC, Hickey JM, Fang G, Salmon ED. Nuf2 and Hec1 are required for retention of the checkpoint proteins Mad1 and Mad2 to kinetochores. *Curr Biol*. 2003; 13:2103–2109. [PubMed: 14654001]
11. Maiolica A, Cittaro D, Borsotti D, Sennels L, Ciferri C, Tarricone C, Musacchio A, Rappsilber J. Structural analysis of multiprotein complexes by cross-linking, mass spectrometry, and database searching. *Mol Cell Proteomics*. 2007; 6:2200–2211. [PubMed: 17921176]
12. Wei RR, Sorger PK, Harrison SC. Molecular organization of the Ndc80 complex, an essential kinetochore component. *Proc Natl Acad Sci U S A*. 2005; 102:5363–5367. [PubMed: 15809444]
13. Hayashi I, Ikura M. Crystal structure of the amino-terminal microtubule-binding domain of end-binding protein 1 (EB1). *J Biol Chem*. 2003; 278:36430–36434. [PubMed: 12857735]
14. Knipling L, Hwang J, Wolff J. Preparation and properties of pure tubulin S. *Cell Motil Cytoskeleton*. 1999; 43:63–71. [PubMed: 10340704]

15. Vorozhko V, Emanuele M, Kallio M, Stukenberg P, Gorbsky G. Multiple mechanisms of chromosome movement in vertebrate cells mediated through the Ndc80 complex and dynein/dynactin. *Chromosoma*.
16. Emanuele M, Burke DJ, Stukenberg PT. A Hec of a microtubule attachment. *Nat Struct Mol Biol*. 2007; 14:11–13. [PubMed: 17203069]
17. Joglekar AP, Bouck DC, Molk JN, Bloom KS, Salmon ED. Molecular architecture of a kinetochore-microtubule attachment site. *Nat Cell Biol*. 2006; 8:581–585. [PubMed: 16715078]
18. Hill TL. Theoretical problems related to the attachment of microtubules to kinetochores. *Proc Natl Acad Sci U S A*. 1985; 82:4404–4408. [PubMed: 3859869]
19. Desai A, Murray A, Mitchison TJ, Walczak CE. The use of *Xenopus* egg extracts to study mitotic spindle assembly and function in vitro. *Methods Cell Biol*. 1999; 61:385–412. [PubMed: 9891325]
20. Lan W, Zhang X, Kline-Smith SL, Rosasco SE, Barrett-Wilt GA, Shabanowitz J, Hunt DF, Walczak CE, Stukenberg PT. Aurora B phosphorylates centromeric MCAK and regulates its localization and microtubule depolymerization activity. *Curr Biol*. 2004; 14:273–286. [PubMed: 14972678]
21. Li L, Yang L, Scudiero DA, Miller SA, Yu ZX, Stukenberg PT, Shoemaker RH, Kotin RM. Development of recombinant adeno-associated virus vectors carrying small interfering RNA (shHec1)-mediated depletion of kinetochore Hec1 protein in tumor cells. *Gene Ther*. 2007; 14:814–827. [PubMed: 17330085]
22. McClelland ML, Gardner RD, Kallio MJ, Daum JR, Gorbsky GJ, Burke DJ, Stukenberg PT. The highly conserved Ndc80 complex is required for kinetochore assembly, chromosome congression, and spindle checkpoint activity. *Genes Dev*. 2003; 17:101–114. [PubMed: 12514103]

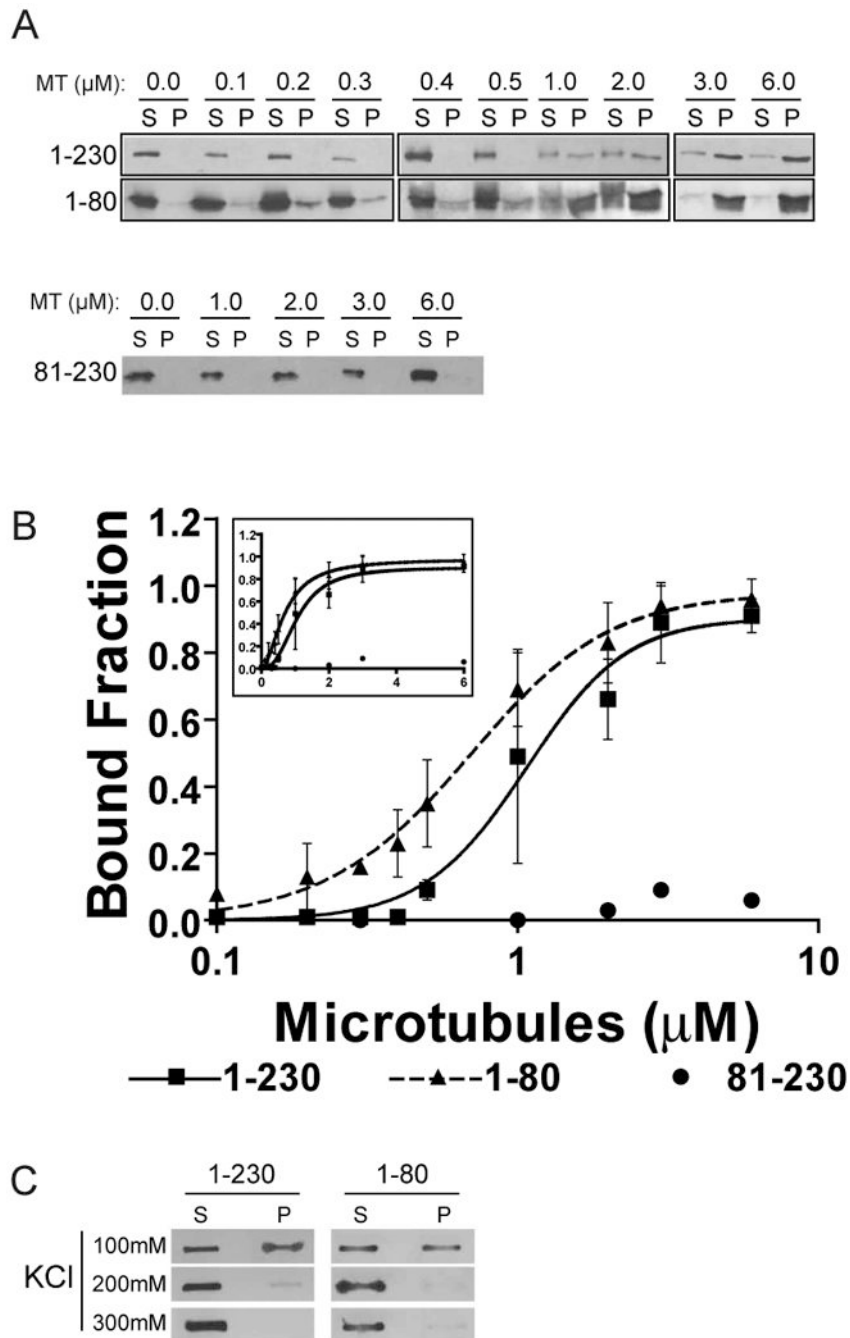


Figure 1. The N-terminal tail of Hec1 binds microtubules (MT) in vitro

(A) The specified Hec1 domains were purified and sedimented with the indicated concentrations of microtubules (MT). Supernatant (S) and pellet (P) samples were collected and subjected to western blot. (B) Hec1 signal intensity from supernatant and pellet samples from three independent experiments were quantified and the mean percentage of Hec1 bound at each microtubule concentration was plotted on a log and linear scale (inset). Also shown is the modified Hill equation binding curve that was fit to the data and used to find apparent K_d values. Hill coefficients were 2.61 ± 0.74 and 1.83 ± 0.24 for Hec1(1-230) and Hec1(1-80), respectively. Error bars indicate standard deviation. (C) A constant concentration of each indicated Hec1 domain and microtubules were sedimented with

increasing concentrations of KCl and the supernatant and pellet samples were analyzed by slot blotting.

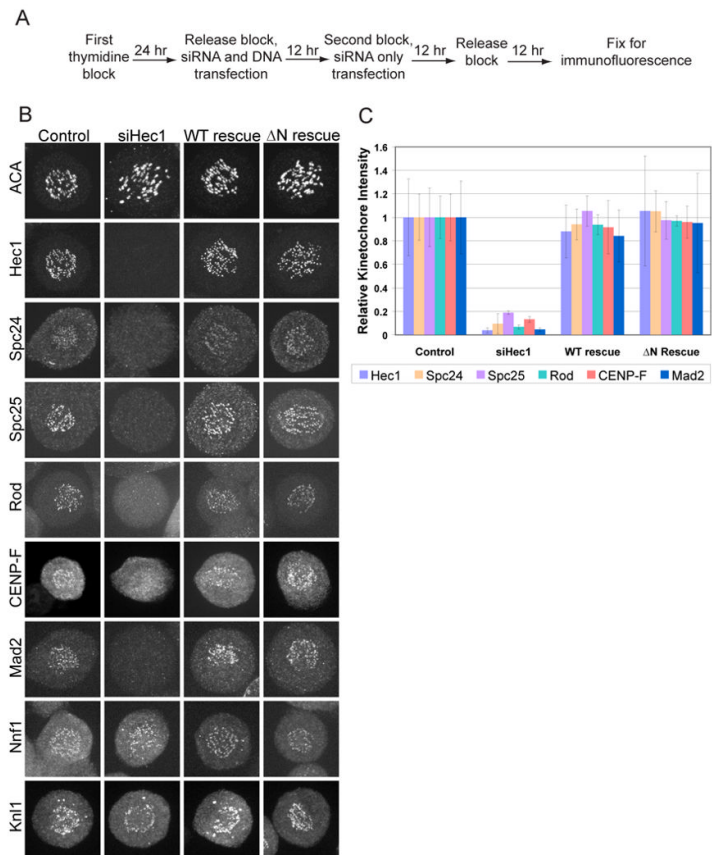


Figure 2. Kinetochores assemble in wild type (WT) and Δ N rescue cells

(A) Scheme used to replace Hec1 in synchronized HeLa cells. (B) Cells were immunostained for the indicated kinetochore proteins. Representative cells for each condition are shown. (C) Kinetochore signal intensity was quantified for all proteins showing a reduction in siHec1-treated cells and expressed as a ratio against the signal intensity of ACA. 10 kinetochores in 10 cells were measured (n=100). All ratios are plotted relative to the control cell mean. Error bars indicate standard deviation.

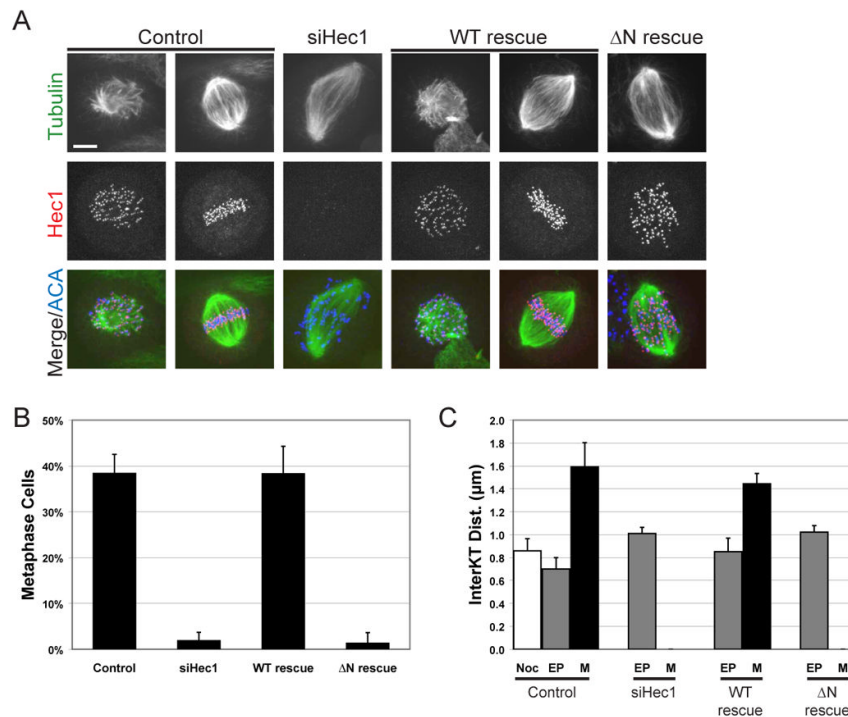


Figure 3. The N-terminal tail of Hec1 is required for chromosome congression and the generation of interkinetochore tension

(A) Cells were immunostained for tubulin, Hec1 and ACA. Representative prometaphase and metaphase cells are shown for control and WT rescue. Only prometaphase cells are found in siHec1 and ΔN rescue cells. Bar = 5μm (B) Mitotic cells were scored for kinetochore alignment in three independent experiments (n=300 for each condition) and the mean percentage of metaphase cells was plotted. (C) 10 sister kinetochores in 10 cells (n=100) were identified by ACA staining between Hec1 signal and the distance measured in three independent experiments. The mean distance is plotted for nocodazole-treated control cells (Noc), early prometaphase (EP) and metaphase (M). Error bars indicate standard deviation.

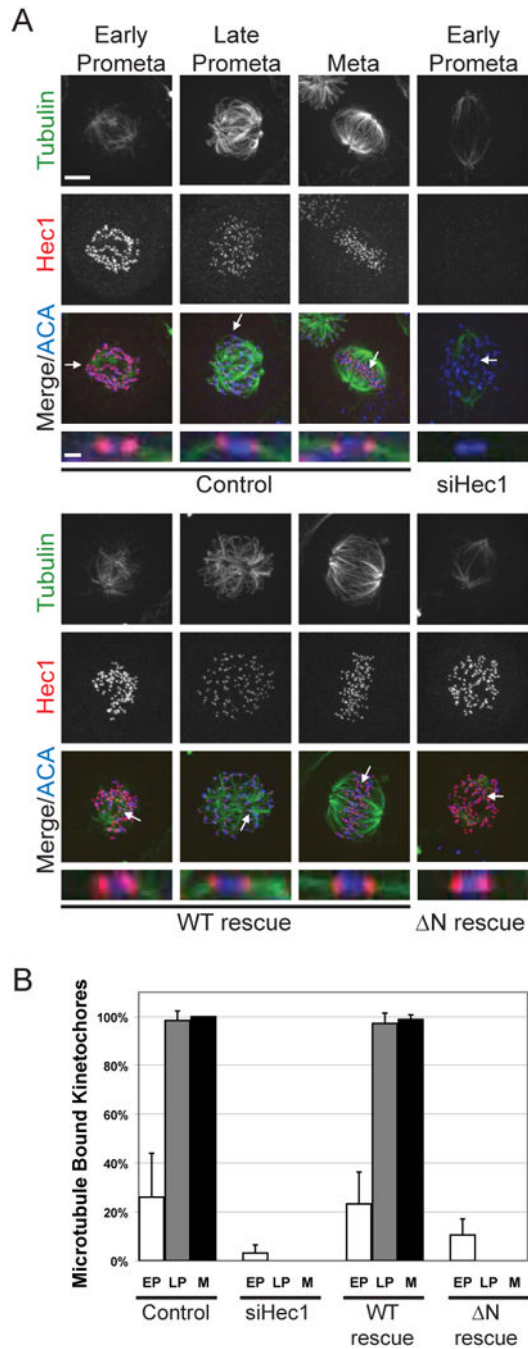


Figure 4. The N-terminal tail of Hec1 is necessary for establishing cold-stable microtubule attachments

(A) Cells were incubated in ice-cold media for 10 min before fixation and immunofluorescence. Representative cells from each mitotic phase are shown as indicated. Arrows point to kinetochores that are enlarged below each merge. Bar = 5 μ m and 1 μ m (B) 10 kinetochores from 5 or more cells ($n > 50$) were scored for associated microtubules in two independent assays and the mean percentage in early prometaphase (EP), late prometaphase (LP), and metaphase (M) was plotted. Error bars indicate standard deviation.